Supplementary Information (SI) for ChemComm.
This journal is © The Royal Society of Chemistry 2026

Supplementary Information (SI)

Enhanced nitrate electroreduction to ammonia on RuRhFeCoNiCu high-entropy oxide nanotubes by constructing oxygen vacancies

Xin Jiang,[#a] Zhixin Wang,[#a] Panyan Chen,[a] Heng Bian,[a] luokai wang,[b] Honghui Wang,*[c] Xinsheng Zhao,*[a] and Lu Wei,*[a]

[a] *School of Physics and Electronic Engineering, Jiangsu Normal University, Xuzhou 221116, China*

[b] *CW CHU COLLEGE，Jiangsu Normal University, Xuzhou 221116, China.*

[c] *Xiamen University Tan Kah Kee College, Zhangzhou 363105, China.*

** Corresponding authors*

E-mail addresses: lwei057@jsnu.edu.cn (L. Wei), xinshengzhao@jsnu.edu.cn (X. Zhao)

whhui2006@163.com (H. Wang)

# X. Jiang and Z. Wang contributed equally to this work.

Experimental Section

Chemical and materials.

Rutheniumchloride hydrate ($RuCl_3 \cdot xH_2O$), potassium hexachlororhodate (K_3RhCl_6), ferric trichloride ($FeCl_3$), cobalt(II) nitrate hexahydrate ($Co(NO_3)_3 \cdot 6H_2O$), nickel chloride hexahydrate ($NiCl_2 \cdot 6H_2O$), copper nitrate trihydrate ($Cu(NO_3)_3 \cdot 3H_2O$), N,N-dimethylformamide (DMF), polyvinylpyrrolidone (PVP, M_w=1300000), potassium sulfate (K_2SO_4), potassium nitrate (KNO_3), hydrogen peroxide solution (H_2O_2, 30%), sulfuric acid (H_2SO_4, 98%) and absolute ethanol were purchased from Sinopharm Chemical Reagent Co. Ltd (China). High purity argon (Ar, 99.999%) gases were purchased from Xuzhou specialty gas Co. Ltd. Nafion solution (5 wt%) was purchased from Sigma-Aldrich Chemical Reagent Co., Ltd. All reagents are analytical grade and used without further purifications.

Synthesis of RuRhFeCoNiCu HEO-NTs with oxygen vacancies.

The RuRhFeCoNiCu HEO-NTs were prepared as follow: Typically, 0.5 g of $RuCl_3 \cdot xH_2O$, 0.27 g of K_3RhCl_6, 0.081 g of $FeCl_3$, 0.15 g of $Co(NO_3)_3 \cdot 6H_2O$, 0.12 g of $NiCl_2 \cdot 6H_2O$, and 0.12 g of $Cu(NO_3)_3 \cdot 3H_2O$ were first dissolved in a 5 mL of DMF and magnetically stirred for 24 h at 40 °C. Then, 0.614 g of PVP was added to the resulting solution and stirred for 24 h at room temperature to form a viscous precursor solution. Subsequently, the prepared solution was put in a 10 ml plastic syringe equipped with a stainless-steel nozzle with an inner diameter of 0.6 mm. A high-voltage power supply of 15 kV was applied between the needle tip and the rotating drum collector at a distance of 15 cm. The syringe pump device was used to maintain the solution at a propulsion rate of 0.015 mm min^{-1}. After the electrospinning process, the resulting fibers were collected and HEO-treated at 70 ℃ for 2 h in a vacuum drying oven. Soon afterwards, the treated fibers were transferred

to muffle furnace, in which the fibers were calcined at 400 ℃ for 3 h under air atmosphere. After calcination, the resulting fibers keep in a quartz tube furnace with N_2/H_2 (10%) mixture carrier gas at 150 ℃ for 0.5 h, and then naturally cooled down to room temperature.

Characterization. The field emission scanning electron microscopy (SEM) images of RuRhFeCoNiCu HEO-NTs were performed on SU8010 electron microscope. Transmission electron microscopy (TEM), selected-area electron diffraction (SAED) patterns and elemental mapping measurements were carried out on FEI Tecnai-F20 transmission electron microscope at 200 kV. The Ru, Rh, Fe, Co, Ni and Cu contents of HEO-NTs were analyzed by energy-dispersive X-ray (EDX) on FEI Tecnai-F20 TEM and inductively coupled plasma-mass spectrometry (ICP-MS, Thermo ICAP-QC). X-ray diffraction (XRD) patterns were collected using an X-ray diffractometer (Rigaku D/MAX 2500 v/pc, Japan) with a Cu Ka radiation source (λ = 1.5406 Å). X-ray photoelectron spectroscopy (XPS) was carried out on an ESCALAB 250Xi spectrometer (Thermo Scientific, USA). The measured value of the electron binding energy was calibrated with respect to the principal peak of C 1s at 284.5 eV as the internal standard.

Preparation of RuRhFeCoNiCu HEO-NTs electrode

5.0 mg of the RuRhFeCoNiCu HEO-NTs and 50 μL Nafion solution (5 wt %) were mixed with 600 μL absolute ethanol and dispersed by ultrasonic treatment for 2 h. Then take 20 μL of the HEO-NTs ink drip onto a GC electrode with a diameter of 6 mm and naturally dried in air. The catalyst loading of the as-synthesized RuRhFeCoNiCu HEO-NTs electrode is 0.15 mg.

Preparation of commercial Ru, Rh, Cu catalysts electrodes

The preparation of commercial Ru, Rh, Cu catalysts electrodes are similar to that of HEO-NTs electrode. Namely, 5.0 mg of commercial catalysts and 50 μL Nafion solution (5 wt %) were mixed

with 600 μL absolute ethanol and dispersed by ultrasonic treatment for 2 h. Then take 20 μL of the catalyst ink drip onto a GC electrode with a diameter of 6 mm and naturally dried in air.

Electrochemical measurements

The NRA tests were conducted in an H-type electrolytic cell containing 1 M KOH + 1 M KNO_3 solution. The saturated calomel reference electrode (SCE) and graphite carbon rod counter electrode were used. The cathodic and anodic chambers of the reactor were separated by Nafion117 that was boiled successively in 5 % H_2O_2, 0.5 M H_2SO_4, and ultrapure water at 80 ℃ for 1 h. High-purity Ar was passed for 2 hours before the test to completely remove O_2 from the electrolyte solution, and passed throughout the NRA reaction. The scan rates for LSV tests were maintained at 20 mV s^{-1}. Chronoamperometry (CA) was performed at various applied potentials (-1.1, -1.2, -1.3, -1.4, -1.5, -1.6 V vs SCE) for 1 h. All the current densities were calculated on the basis of the geometric surface area of working electrode. The gaseousness NH_3 product was collected by 10 mM HCl solution during the electrolysis. The NH_4^+, NO_2^- and N_2H_4 products were detected by UV-Vis spectrophotometer.

Products measurements

NH_4^+ was detected by indophenol blue indicator method: Take 1 mL solution from the cathode chamber, then add 1 mL of 10 mM HCl solution for acidification, 2 mL solution containing 1 M sodium hydroxide, 5 wt% sodium citrate and 5 wt% salicylic acid, 1 mL NaClO solution and 0.2 mL nitrofuran solution, respectively. The absorbance at 656 nm was measured after 1 hour at room temperature.

The yield rate ($R_{(NH3)}$) and Faraday efficiency (FE) of product NH_3 were calculated as follows:

$$R(NH_3) = \frac{\left[NH_4^+\right] \times V}{t \times m_{cat}}$$

$$FE_{NH_3} = \frac{Q_{NH_4^+}}{Q_{total}} = \frac{8 \times 96500 \times \left[NH_4^+\right] \times V}{M_{NH_4^+} \times \int idt}$$

[NH_4^+] is the concentration of NH_4^+ in the cathode chamber solution after electrolysis for 1 hours, V is the volume of electrolyte solution in the cathode chamber, t is the electrolytic time of 1 hours, Q_{NH4^+} is the electricity consumed by the generation of NH_4^+ for 1 hours of electrolysis, and Q_{total} is the electricity consumed in 1 hours of electrolysis.

Determination of NH_4^+ concentration standard curves: Detect the absorbance at 656 nm of 1 M KOH + 1 M KNO_3 solution standard solutions with different NH_4^+ concentrations. The absorbance - NH_4^+ concentration relation curve was obtained by linear fitting each concentration with the corresponding absorbance, as shown in Figure S10.

Preparation of NO_2^- indicator: 4 g p-aminobenzene sulfonamide and 0.2 g N-ethylenediamine hydrochloride were dissolved in 50 ml water and 10 ml phosphoric acid to make a lavender translucent solution.

Detection of NO_2^-: Mix 5 mL solution from the cathode chamber with 0.1 mL indicator. The absorbance at 540 nm was measured after 1 hour at room temperature.

The Faraday efficiency of NO_2^- was calculated as follows:

$$FE_{NO_2^-} = \frac{Q_{NO_2^-}}{Q_{total}} = \frac{2 \times 96500 \times \left[NO_2^-\right] \times V}{\int idt}$$

[NO_2^-] is the concentration of NO_2^- in the cathode chamber solution after electrolysis for 1 hours, V is the volume of electrolyte solution in the cathode chamber, t is the electrolytic time of 1 hours, Q_{NO2^-} is the electricity consumed by the generation of NO_2^- for 1 hours of electrolysis, and Q_{total} is the electricity consumed in 1 hours of electrolysis.

Determination of NO_2^- concentration standard curves: Detect the absorbance at 540 nm of 1 M KOH + 1 M KNO_3 solution standard solutions with different NO_2^- concentrations. The absorbance - NO_2^- concentration relation curve was obtained by linear fitting each concentration with the corresponding absorbance, as shown in Figure S12.

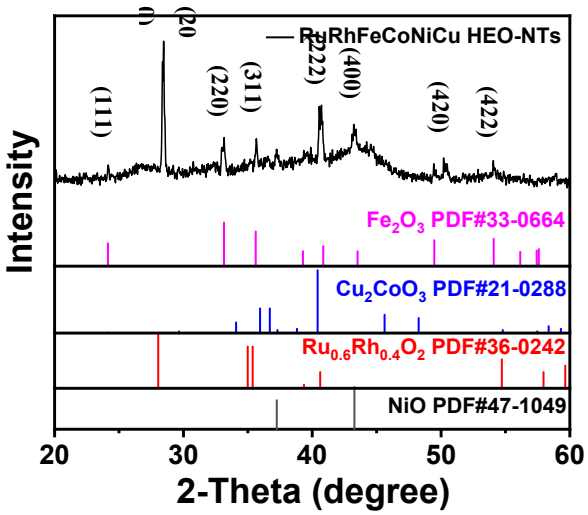

Fig. S1. XRD curves of RuRhFeCoNiCu HEO-NTs.

Fig. S1 shows XRD curves of RuRhFeCoNiCu HEO-NTs and the standard reference patterns. Based on the comparison with reference patterns, we conclude that no diffraction peaks from pure oxide phases are present within the detection limit of XRD. This supports the conclusion that all the HEO elements are homogeneously incorporated into the high-entropy lattice. The small peak shifts observed relative to the reference patterns are attributed to lattice distortion induced by the multiple elements.

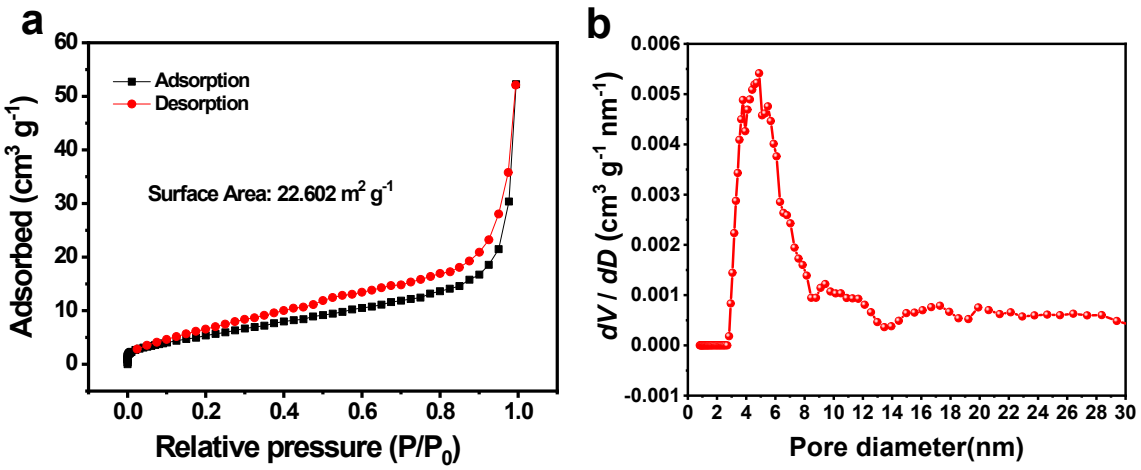

Fig. S2. (a) N_2 adsorption-desorption isotherm and (b) the pore size distribution of RuRhFeCoNiCu HEO-NTs.

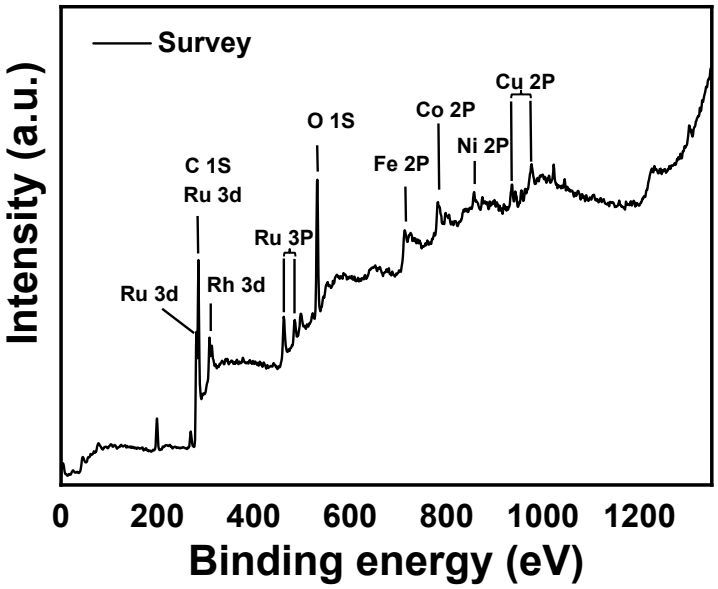

Figure S3. XPS survey spectrum of RuRhFeCoNiCu HEO-NTs.

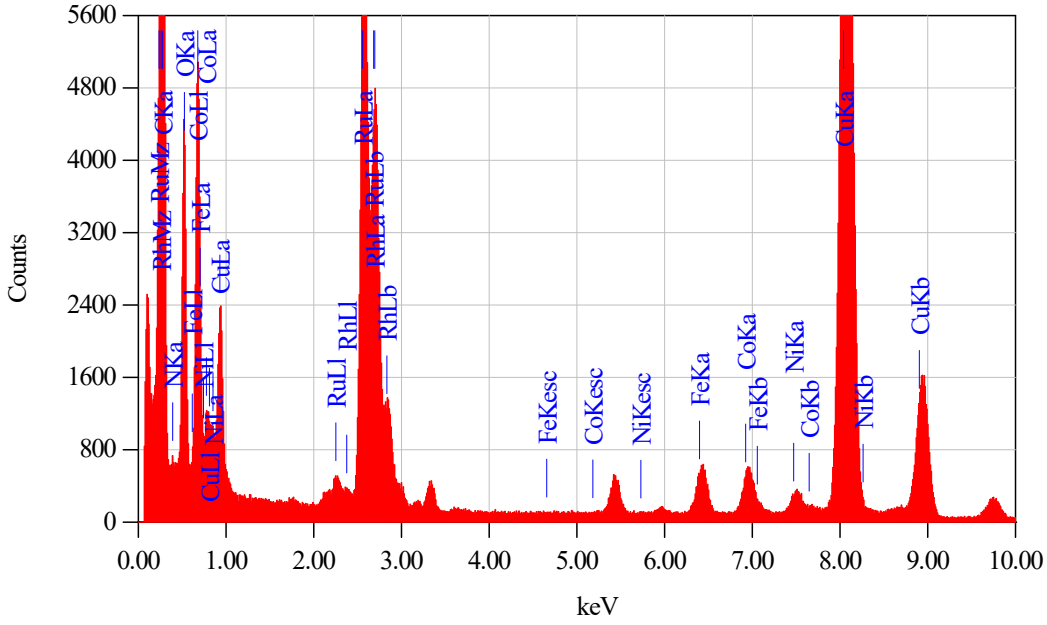

Fig. S4. EDS spectrum of RuRhFeCoNiCu HEO-NTs.

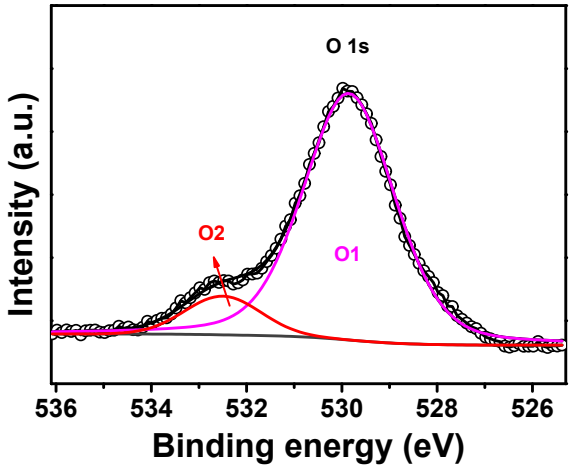

Fig. S5. High resolution O 1s XPS of RuRhFeCoNiCu HEO-NTs without H_2 treatment.

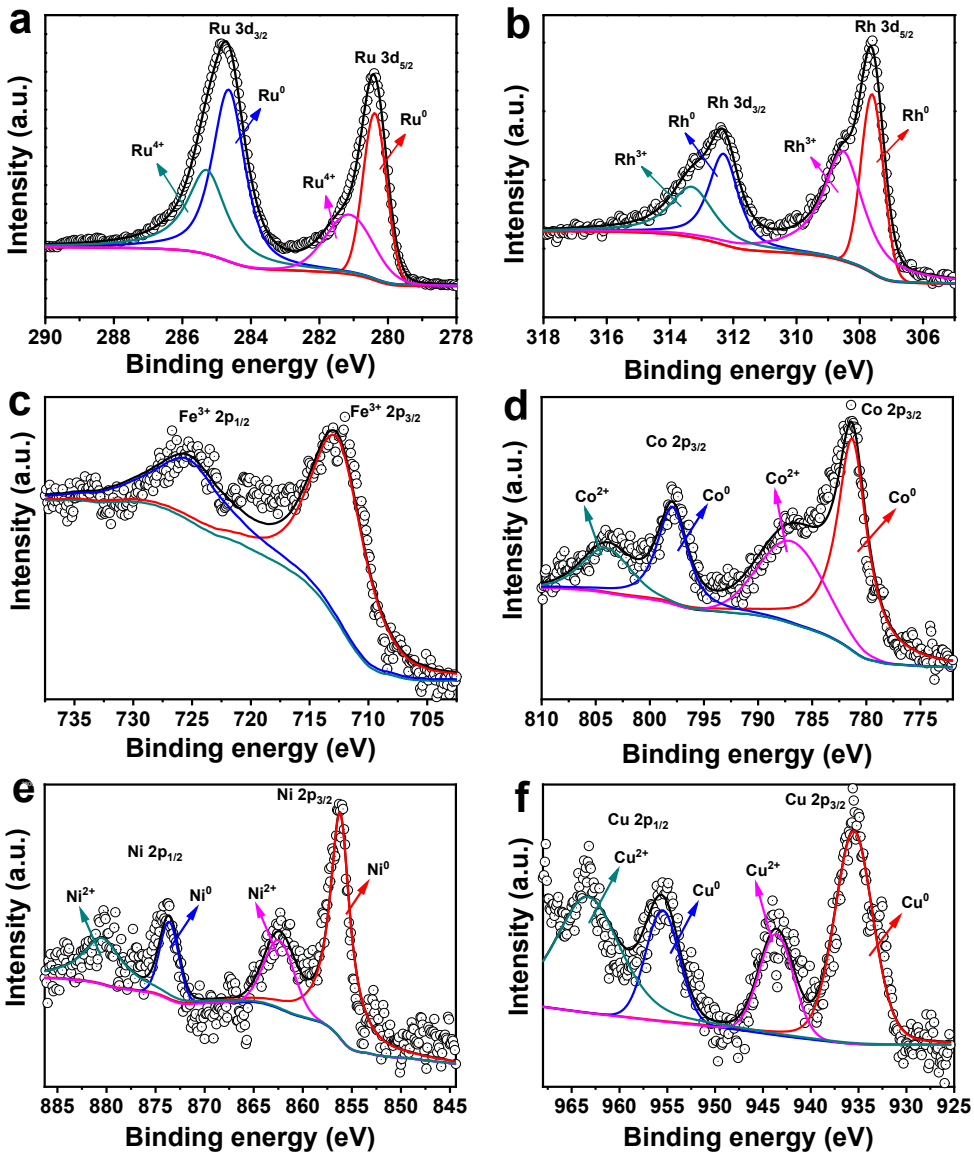

Fig. S6. High resolution XPS spectra of RuRhFeCoNiCu HEO-NTs: (a) Ru 3d, (b) Rh 3d, (c) Fe 2p, (d) Co 2p, (e) Ni 2p, (f) Cu 2p.

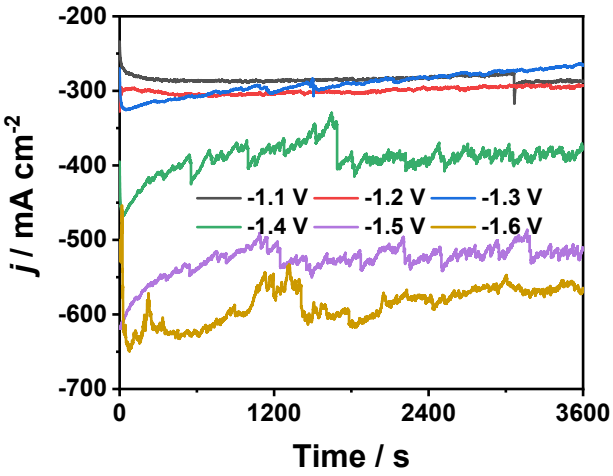

Fig. S7. *i-t* curves at various applied potentials.

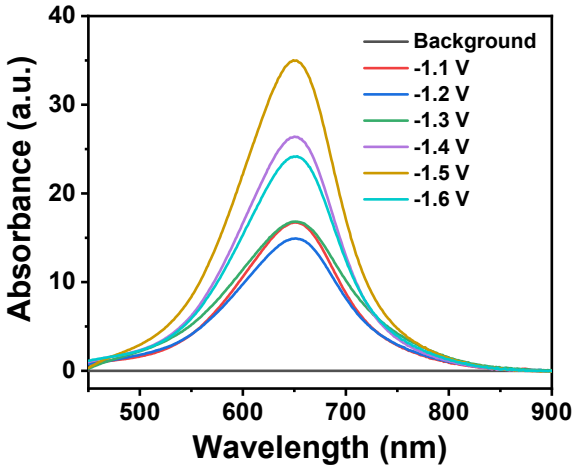

Fig. S8. UV-vis absorption spectra of electrolytic solutions at various applied potentials measured by indophenol blue indicator method.

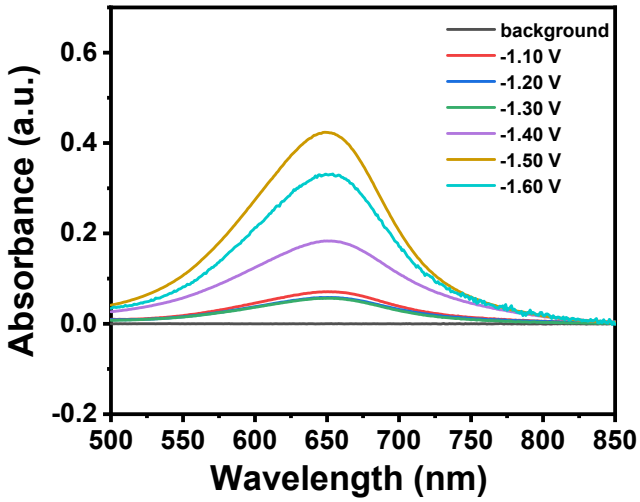

Fig. S9. UV-vis absorption spectra of the collecting tail gas solutions at various applied potentials measured by indophenol blue indicator method.

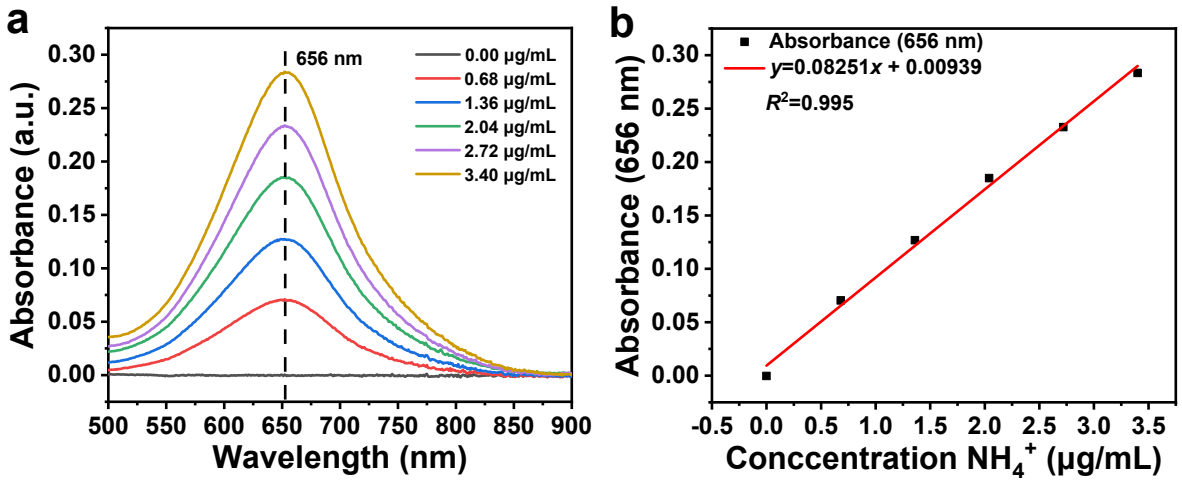

Fig. S10. (a) UV-vis absorption spectra of standard solutions with different concentrations of NH_4^+. (b) Linear relationship between absorbance and concentration of NH_4^+: $y = 0.08251x + 0.00939$, $R^2 = 0.995$.

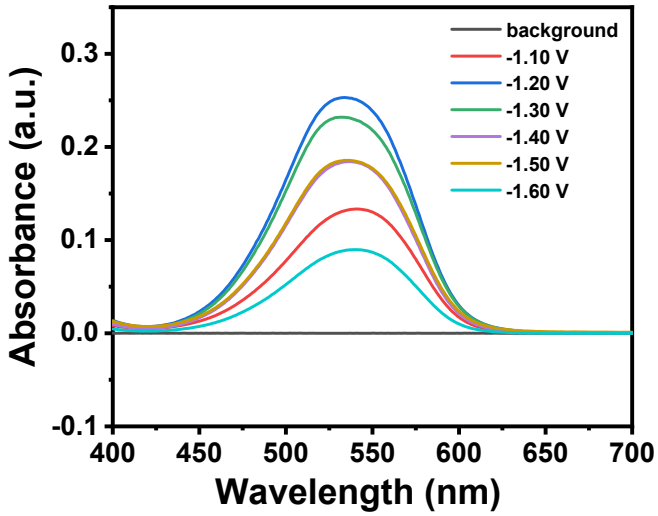

Fig. S11. UV-vis absorption spectra of NO_2^- in electrolytic solutions at various applied potentials.

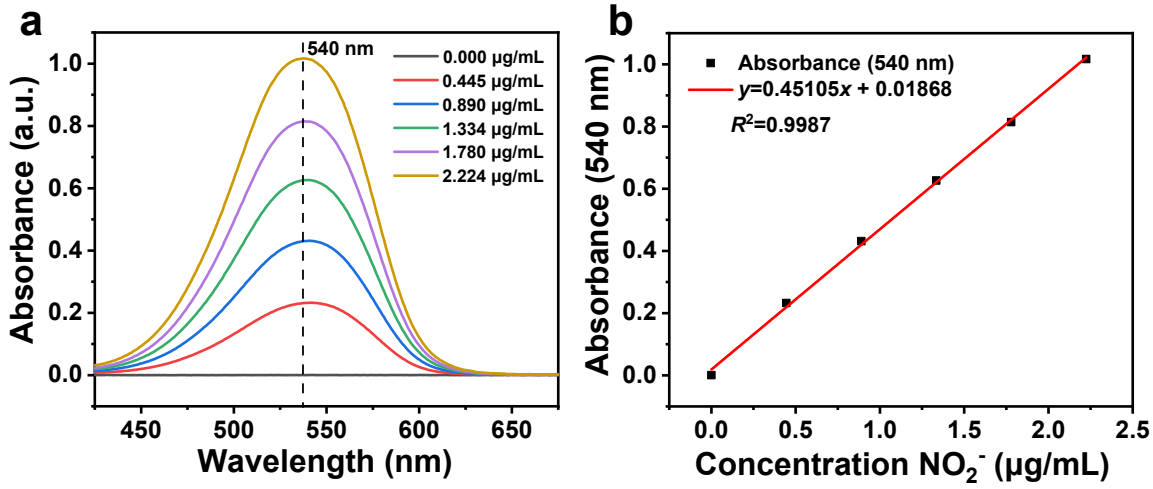

Fig. S12. (a) UV-vis absorption spectra of standard solutions with different concentrations of NO_2^-. (b) Linear relationship between absorbance and concentration of NO_2^-: $y = 0.45105x + 0.01868$, $R^2 = 0.9987$.

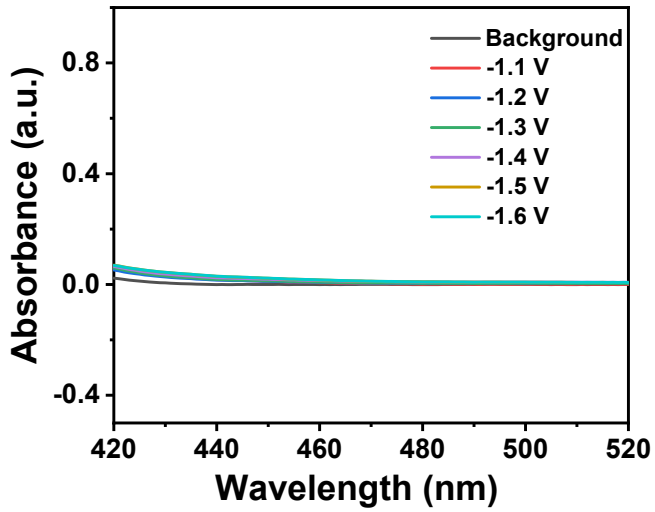

Fig. S13. UV-vis absorption spectra of N_2H_4 in electrolytic solutions at various applied potentials measured by Watt and Chrisp method.

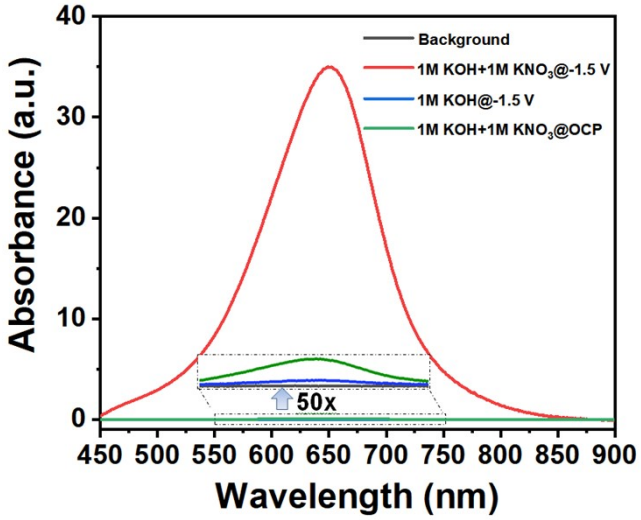

Fig. S14. UV-vis absorption spectra of the electrolytes stained with the indophenol indicator under different conditions. Inset is the absorption intensity with 50 times magnification of the area in the dashed box.

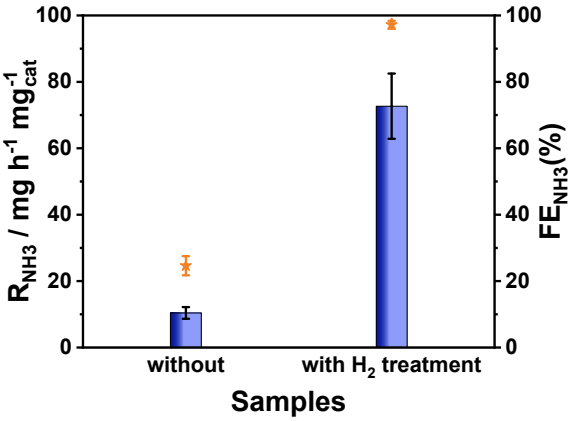

Fig. S15. Comparison of R_{NH3} and FE_{NH3} at -1.5 V (vs. SCE) on RuRhFeCoNiCu HEO-NTs without and with H_2 treatment.

Fig. S15 compares the NRA performance (R_{NH3} and FE_{NH3}) of the RuRhFeCoNiCu HEO-NTs without and with H_2 treatment. The untreated sample exhibits substantially lower NH_3 yield (R_{NH3}) and Faradaic efficiency (FE_{NH3}) compared to the H_2-treated sample. For example, at -1.5 V vs. SCE, the untreated sample gives an R_{NH3} of only 10.4 mg h^{-1} $mg_{cat.}^{-1}$ and a FE_{NH3} of 24.6%, whereas the H_2-treated sample reaches 72.7 mg h^{-1} $mg_{cat.}^{-1}$ and 97.2% under the same conditions. These control experiments clearly show that the introduction of OVs via H_2 treatment greatly enhances the NRA activity.

Table S1. Comparison of the NH_3 yield rate and FE on the advanced high-entropy catalysts for NRA.

Entry	Catalysts	Electrolytes	NH_3 yield	FE / %	Refs.
1	RuFeCoNiMnMo	0.5 M K_2SO_4 + 0.1 M KNO_3	83.35[a]	99.3	Adv. Mater. 2026, 38, e21096
2	RuPdCoCuZn	0.1 M KOH + 0.1 M KNO_3	20.95[b]	>90	Angew. Chem. Int. Ed. 2026, 65, e20035
3	$(CoMnFeNiCu)_3O_4$	1.0 M KOH + 0.1 M KNO_3	1.83[b]	96.3	Adv. Mater. 2025, 37, e08982
4	MnFeCoNiCu	0.5 M Na_2SO_4 + 0.1 M NO_3^-	10.2[a]	94.5	Adv. Mater. 2025, 37, 2415739
5	HEA-RE	0.5 M K_2SO_4 + 200 ppm M KNO_3	0.215[d]	~99	Angew. Chem. Int. Ed. 2025, 64, e202515842
6	CoNiCuMnFe	0.1 M KOH + 0.05 M NO_3^-	3.25[c]	92	Adv. Funct. Mater. 2025, 35, 2415970
7	FeCoNiGeSb-HEI	1.0 M KOH + 500 ppm NO_3^-	7.5[c]	97.6	Angew. Chem. Int. Ed. 2025, 64, e202502333
8	HEAOs	1.0 M KOH + 0.5 M KNO_3	0.314[d]	84	Small 2026, 22, e07803
9	FeCoNiAlTi	0.2 M $K2_SO_4$ + 50 mM KNO_3	0.52[c]	95.23	Angew. Chem. Int. Ed. 2024, 63, e202407589
10	FeNiCoMnRh	0.5 M NaOH + 0.25 M NO_3^-	0.0754[d]	81.5	Chem. Eur. J. 2025, 31, e202500887
11	CuCoNiRuPt	1 M KOH + 1000 ppm KNO_3	3.4[d]	98	Nano Lett. 2025, 25, 14185
12	PdCuNiCoZn	0.5 M K_2SO_4 + 0.1 M KNO_3	447[a]	99.0	Nat. Commun. 2025, 16, 7915
13	np-CuCoNiPdRuAl	0.1 M KOH + 50 mM NO_3^-	30.47[a]	97.4	Sci. China Chem. 2026, 69, 1233
14	MgCoNiCuZnO	1 M KOH + 0.1 M KNO_3	4.48[a]	93.4	Nat. Commun. 2024, 15, 260
15	HE-OH	1 M KOH + 0.1 M KNO_3	30.4[c]	~100	Chinese Chem. Lett. 2025, 36, 111294
16	CuNiCoZnMn	0.5 M Na_2SO_4 + 0.1 M KNO_3	0.7237[d]	96.6	ACS Appl. Mater. Interfaces 2024, 16, 43526
17	HESA NCs	0.5 M Na_2SO_4 +100 mM $NaNO_3$	81.4[a]	93.4	Nat. Commun. 2024, 15, 6932
18	FeCoNiCuRu	0.5 M K_2SO_4 + 0.1 M KNO_3	0.84145[c]	94.5	Chem. Eng. J. 2024, 500, 157426
19	FeCoNiCuSn HEA/rGO/CP	0.1 M Na_2SO_4 + 100 ppm $NaNO_3$	0.8837[c]	94.5	Inorg. Chem. Front., 2025, 12, 682
20	RuRhFeCoNiCu HEO-NTs	1.0 M KOH + 1.0 M KNO_3	72.7[a] / 2.3[d]	97.2	This work

Note: [a] mg h^{-1} $mg_{cat.}^{-1}$; [b] mmol h^{-1} $mg_{cat.}^{-1}$; [c] mg h^{-1} cm^{-2}; [d] mmol h^{-1} cm^{-2}